ISSN: 0974-5823 Vol. 7 No. 1 January, 2022

International Journal of Mechanical Engineering

Design of a Hybrid Haptic Wearable Device for Upper Limb Amputees to Recover the Missing Sensation

Abdullah I. Abdullah[1,2], Norasikin Mat Isa[1], Mohammad A. Al-Mashhadani[2], O. M. Al-Moayed[1], A. K. Kareem[1,3]

[1]Faculty of Mechanical and Manufacturing Engineering, University Tun Hussein Onn Malaysia, 86400 Parit Raja, Batu Pahat, Johor, Malaysia.

[2]Department of Computer Technique Engineering College, Al-Maarif university college Ramadi, Anbar, Iraq.

[3]Department of Biomedical Engineering, Al-Mustaqbal University College, Babylon, Iraq.

Abstract— The hybrid haptic feedback motivation system which is able to sense the surface texture, and the temperature, simultaneously, a prosthetic hand was modeled to achieve the tangible impression to resection patients. Moreover, the haptic system was designed to facilitate withdrawal reactions in users of the prosthetic device in response to thermally noxious stimuli. Through non-invasive stimulation of the skin residual limbs, re-sensation is achieved depending on the type and the level of tactile signals provided by the prosthetics' sensory system. Consequently, An innovative hybrid pressure-vibration-thermal feedback stimulation system was designed to give the users a lot of information regarding the prostheses environment without requiring long pre-training or brain confusion. The assessment of response and sensation executed on hygienic volunteers to gauge the system capability to encourage the nerve system of the human. As indicated by the results and volunteers' responses, amputees can feel contact pressure, surface texture, and object temperature as well as perform thermal withdrawal reflexes by using the solution developed in this study.

Keywords— Feeling recovering, Haptic feedback stimulation system, Contact pressure detection, Surface texture detection, Temperature detection, Upper limb prostheses, Prosthetic hand, Implementing withdrawal reflex.

1. Introduction

Despite the rapid progress in medical science in recent decades, the quality of life for patients with upper limb amputations has barely changed [1]. In fact, those who were amputationed thought they were still using hooks on the ends of their arms as upper limb prostheses [2]. According to a statistical study on 2477 amputees who have had their upper limbs amputated [3], typical upper limb prostheses have the following basic requirements:: (i) Provide the users with less visual attention needed to perform their daily activities, (ii) As much as possible, allow the patients to manipulate different objects of different sizes, and (iii) Create a prosthetic hand that appears and functions the most like a healthy human hand possible. However, the lack of exteroception and proprioception information makes the control on the upper limb prostheses more difficult [4,5]. Nowadays, numerous studies are being conducted in order to overcome the challenges of a lack of sensation during use of prostheses and allow amputees to learn about their environment through their prosthetic hands[6].

The loss of touch can make it especially difficult for amputees with prosthetic hands to hold and manipulate objects, especially when the task requires a certain amount of skill and tactile feedback. In this case, the amputees will not be able to decide how much the hand must open or close, or to determine the strength of the grasp force. The high applied grasping force leads to damaging or trashing of the grasped object, while the light force causes the object to slip out of the hand. Through the same point of view, the inability of the amputees to perceive the surface texture and temperature sensations through their own prostheses deprives them of getting a wealth of information about the environment around them. Without the surface texture sensation, it would be very hard to identify the types and the kinds of the surfaces. Furthermore, the absence of temperature sensitivity leads to prevent the amputees from useful tactile information such as material discrimination, extreme temperature avoidance, and psychological comfort. In addition, the lack of temperature feedback may cause damage to the prostheses through exposure to high temperatures without the knowledge of the users.

This condition is primarily due to developments in prosthetic technology being geared more towards improving actuation, dexterity, and control [7-9], with less work directed at providing feedback channels outside of vision [10, 11]. Moreover, researchers in literature investigated several issues related to the equipping the artificial prosthetic hand with the haptic feedback stimulation system. Firstly, issues related to the problems that make the amputees feel uncomfortable as they use the haptic prosthetic hand, like the heavyweight [12], the high noise level of the actuators [13], and the sensation is absent through prostheses [14] were investigated. A second issue is the increase in energy consumption caused by the auxiliary equipment of the haptic feedback stimulation system [15, 16]. Besides, issues concerned with the examination of how the brain can perceive and analyze simultaneous multi-sensory information obtained by the patient [17], for example, when using two or more different type of sensors lead to the reduction of the recognition accuracy. Finally, issues regarding the deficiency of design of a haptic prosthetic hand having the ability to accomplish all the sensory tasks and functions comparable to the human real hand, for instance, lack of the ability for implementing a withdrawal reflex due to the painful noxious stimulus [18] were also discussed. Overall, haptic feedback stimulation systems have three main disadvantages: (i) patient's brain may get confused due to the massive amount of data sent from the sensory system during the operating of hand prostheses, (ii) the need of long hours of pretraining on how to recognize the sensory information, (iii) the prosthetic's user is unable to perform entire tasks due to the prosthetic design limitation.

Numerous studies have been conducted to find the most appropriate type of haptic feedback display. In general, two types of displays have been compared, such as the comparison of rotating and linear vibration actuators or the comparison of vibrations and skin-stretching wearables, to convey sensory information to amputees with high accuracy and response [12, 19]. On other hand, various studies suggested that combining two or more haptic feedback displays can improve the performance of wearable haptic devices [16, 20-23].

The existing studies mainly investigated the ability to enhance the performance of the prosthetic arm by mean of recovering only one type of the missing sensation using one type of feedback stimulator, for instance, detecting the contact pressure by using a pressure sensor and vibration stimulators. Nevertheless, there appears to be no clear research on the ability of recovering the entire missing sensation by using a hybrid feedback stimulation system without brain confusing, in addition to producing a functional prosthetic arm, which has the ability to perform multitasks similar to a healthy human arm. However, this gap, in particular, has not been investigated clearly in the existing literature. Therefore, due to this, a study is required to design and evaluate a hybrid haptic feedback stimulation system to qualify the upper limb mutilation amputees to distinguish surrounding environment easily without causing any kind of brain confusing or long pre-training requiring. In addition, such system will be able to detect the thermal noxious stimulus which enables the amputees to implement a withdrawal reflex in a quick manner.

The aim of this study can be divided into two main objectives. The first objectives is to enable amputees for recognizing the multi tactile sensation by using the hybrid haptic feedback stimulation system without confusion or long pre-training requiring. While the second objective is to develop a new functionality for detecting the thermal noxious stimulus by using the hybrid haptic feedback stimulation system, which is responsible of enabling the amputees to implement withdrawal reflex quickly. Therefore, the hybrid feedback wearable device was fabricated from the combination of the servomotor to produce a pressing force on the user's skin for the contact pressure indication, vibration motors to recover the sensation of the surface texture, and Peltier element to feed the thermal tactile sensor information. While, the entire parts of the hybrid feedback wearable device were programmed to operate together at the unsafety high-temperature case, to fastly inform the user to implement a with drawl reflex.

2. Modelling of the hybrid wearable device

A haptic wearable device consists of two distinct hybrid haptic systems: the hybrid haptic pressure-vibration feedback stimulation system (HHPVFSS) and the hybrid haptic surface texture-thermal feedback stimulation system (HHTTFSS). In general, the HHPVFSS is similar to the model proposed in the previous study [24]. The HHPVFSS consists of a pair of motors with 10 mm diameter; circular vibration and a single servo motor were used simultaneously, In order to stimulate the amputee's nervous system by applying pressure and vibration to his upper arm's skin, as shown in Figure 1.

For the HHTTFSS described in Figure 1, the vibration motor was fixed inside the plastic cylindrical case, in order to increase the contact area between the effective vibrational surface and the patient's skin. Meanwhile, a piezoelectric Peltier element was inserted inside the plastic rectangular case to perform the thermal feedback stimulation display. The Peltier element, which is a thermoelectric component, is a device that can pump heat from its cold side to the hot side depending on the direction of the current. Therefore, it is a kind of heat pump of solid state. The amount of heat transfer, which can be pumped by this device, certainly depends on the electrical power supplied to it [25].

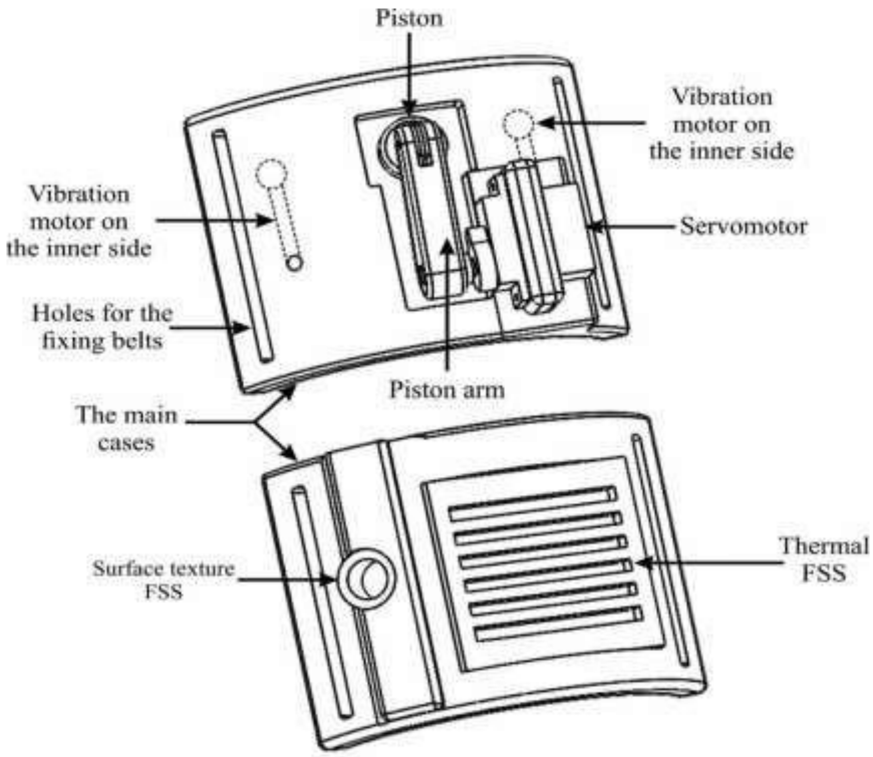

Figure 1: Layout of the hybrid wearable device.

3. Manufacture of the hybrid haptic wearable device

The hybrid haptic wearable device is composed of two split curvature cases. The upper case represents the hybrid haptic pressurevibration feedback stimulation system (HHPVFSS), while the lower case indicates the hybrid haptic surface texture-temperature feedback stimulation system (HHTTFSS). For the two devices, the Solidworks 2018 CAD computer program was used for the design, analysis, and evaluation of the wearable devices. The second fabrication stage is to print the parts by utilizing a 3D printer of type Raise-3D-N2-Plus [26], using Acrylonitrile Butadiene Styrene (ABS) material [27], while the next stage involved smoothing and polishing the printed parts, connecting it using aluminum screws and glues, and finally installing the driving the motors. Lastly, programming and interfacing the electronic pieces of equipment using Matlab 2018b code, and Matlab 2018b / Simulink modified by Simulink support package for Arduino hardware represents. Therefore, the programming code of interfacing the microcontroller computer system was initially generated by Matlab 2018b / Simulink support package for Arduino hardware, then, transferred to C++ code during the building process.

3.1 Fabrication of the hybrid haptic pressure-vibration feedback stimulation system (HHPVFSS)

A combination of pressing and vibration actuators was incorporated into a curved enclosure [13] to transmit the sense of the contact force registered in the pressure sensing system. The fastening belts were lightly wrapped over the volunteer's upper arm. The pressure FSS is represented by a small and lightweight servomotor with a high output power and a piston arm of 40 mm length and a circular piston of 15 mm diameter. The SG-90 servomotor was chosen as the pressure FSS's driver because it has a small weight of 14.7 g, a torque of 2.5 kg.cm, and a voltage range of 4.8 to 6 [28]. These characteristics are ideal for a haptic wearable device. To incorporate the vibration FSS, two vibration motors equipped with linear resonant actuators (LRA) were attached to the interior of the main casing. In this field of research, vibration motors are advantageous because of their low power consumption, low noise, light weight, and excellent performance [29].

The hybrid haptic pressure-vibration feedback stimulation system (HHPVFSS) will stimulate the upper arm of the user as quickly as feasible as the prosthetic hand contacts or grips objects, the pressure increases, by providing a mutual pressure and vibration sensation. The angular location of the servomotor enhances the pressure feeling. As a result, the pressure exerted by the piston on the user's skin increases, while the vibration feeling develops as the providing Pulse-Width Modulation increases (PWM). As a result, the patient will be able to detect changes in the frequency of vibration excitation. Generally, the HHPVFSS aids in the recovery of touch sensations, including start, end, grab, sliding, and contact pressure level. In addition, the HHPVFSS is important in swiftly exciting the amputee's brain during a hot painful stimulation condition.

3.2 Fabrication of the hybrid haptic surface texture-temperature feedback stimulation system (HHTTFSS)

The hybrid haptic surface texture-temperature feedback stimulation system (HHTTFSS) is fabricated from the main case, surface texture FSS, and thermal FSS. The main case is a curvature wearable case of 70 cm length and 10 mm thickness, as displayed in Figure 3. The haptic device was installed on the user's upper arm using the attaching belts to maintain direct contact between the actuators and the user's skin.

The vibration FSS is composed of a circular miniature vibration motor that fits to a cylindrical 3D printed case with 15 mm output diameter. The cylindrical case was connected coaxially within the rigid main case by mean of an aluminum bar of 3 mm dimeter. This type of connection allows the vibration FSS to operate freely without any friction with the main case that leads to a change in the frequency of the vibration FSS, and then a change in the surface texture sensation. A single DC vibration motor of Linear Resonant Actuator (LRA) type with 10 mm diameter was used to deliver vibration at a frequency of 250 Hz [29].

In addition, Figure 3 presents the fabrication of the thermal FSS developed in this study. This device has a Peltier element inserted into a rectangular 3D printed case. The rectangular case, of dimensions 48 × 48 × 11 mm, has an open side to make the Peltier element in direct contact with the user’s skin and a heat sink at the other side for high heat dissipation efficiency. The device is mounted on the user's upper arm in contact with the arm’s skin, in order to transfer the temperature sensation to the prosthetic arm’s user corresponding to the temperature detected by the temperature sensor by regulating the applying input voltage. The TEC1-12706 Peltier element made by HB Brand Electronic Components [30] was used in this study. The maximum performance specifications of the proposed element are 66 °C temperature at 6.4 Amps and 14.4 V.

The essential advantages of the TEC1-12706 Peltier element are low noise and no maintenance required because it is a solid state, i.e. do not possess any moving parts, as well as having a long service lifetime. Meanwhile, the instability behavior of the element presents the main disadvantage side. In other words, it is impossible to set the hot face of the Peltier element within a specific point of temperature. Thus, the temperature degree of the hot side keeps increasing when a constant supplied voltage is used.

Therefore, a voltage regulator control system was designed and tested to control the temperature of the Peltier element within a desired temperature, as shown in Figure 4. The voltage regulator was used to adjust the supplying voltage to the element by adjusting its potentiometer. Voltage regulators supply a constant DC output voltage that is continuously maintained at the desired level regardless of the output voltage setting [31]. The SG-90 servomotor was connected by a hollow cylindrical plastic shaft to the voltage regulator’s potentiometer, in order to automatically control it by mean of the computer and Arduino Mega microcontroller. For safety operation condition and to assure that the skin of the user’s upper arm do not get burn during the thermal excitation, a single channel DC relay module of operating voltage 5-12 V [32] was connected to the control board. The main function of the relay is to open and close the providing power supply to Peltier element at high response.

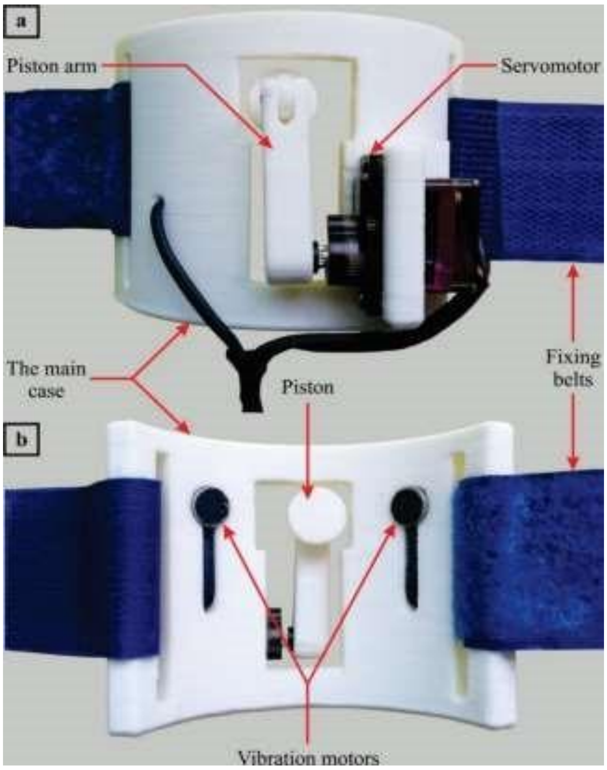

Figure 2: Manufacture of the HHPVFSS:

(a) front view, (b) inner part view.

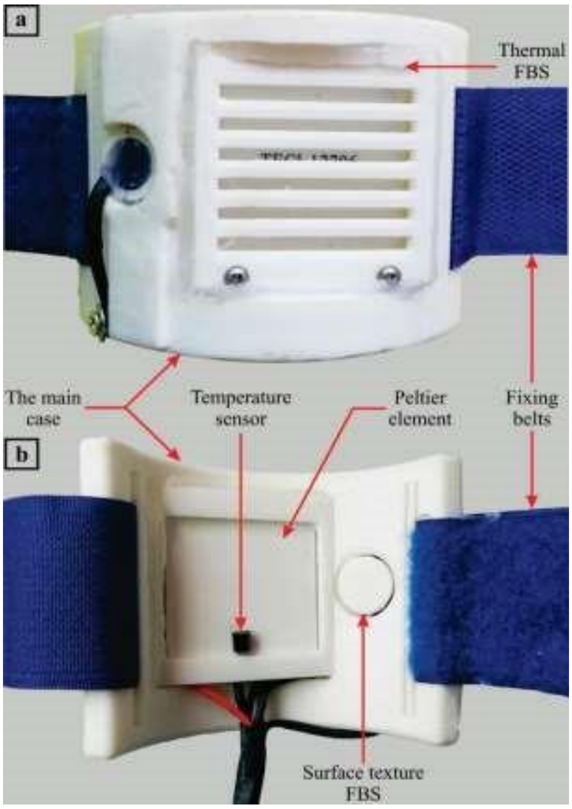

Figure 3: Manufacture of the HHTTFSS:

(a) front view, (b) inner part view.

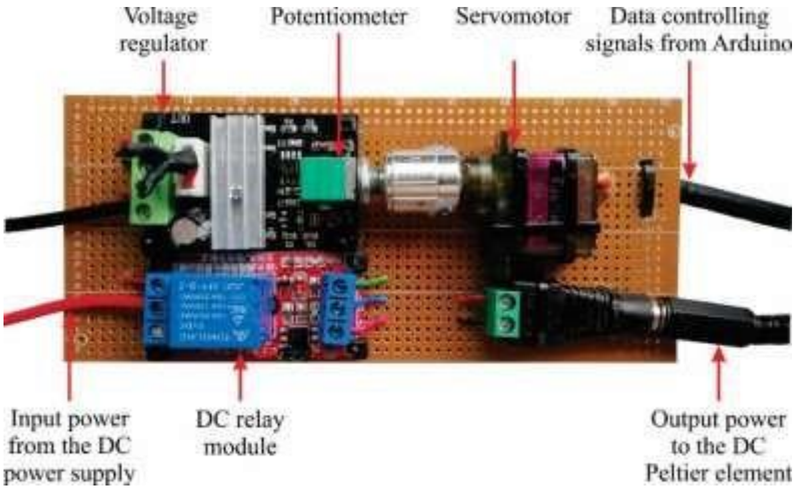

Figure 4: Voltage regulation and control board.

Thus, the relationship between the regulator output voltages against the servomotor angular position must be calculated, in order to exactly control the input and the output voltage to the voltage regulator board by controlling the servomotor angular position. In the experiment, an external DC power supply was used to deliver a constant 8 V to the board, while a digital LCD voltmeter was connected directly on the output terminals of the board to measure the output voltage. The Matlab/ Simulink computer program was directed on the servomotor to change its position gradually, 20 degrees increment in every step. Figure 5 presents the output results of the evaluation experiment. Accordingly, To fit a fitting curve with R-square equal to 0.998, a polynomial fitting equation of fourth degree order was selected:

$$V_f = P_1 \times SP^4 + P_2 \times SP^3 + P_3 \times SP^2 + P_4 \times SP + P_5 \quad (1)$$

Where: V_f and SP describe the voltage fitting value and angular position of the servomotor, respectively, while the values P_{1-5} are the constants of the fitting equation, which equals to $P_1 = 7.213 \times 10^{-9}$, $P_2 = -3.014 \times 10^{-6}$, $P_3 = 0.0004441$, $P_4 = -0.0008362$, and $P_5 = 2.052$.

During the operation of the thermal feedback stimulation system, the Peltier element's temperature must be proportional to the measured temperature signal (T_s) provided from the tactile temperature sensors of the prosthetic hand. Therefore, the desired set point generation required for the relay module (R_d) and Peltier element's temperature (T_d) depends on the tactile temperature signal, as schematized in the black diagram described in Figure 6. The relay module desired signal (R_d) varies only between two values, one to open the circuit at the active time and zero to close it. This implies that the relay module output signal (R_m) will be either 0 V or 8 V depending on the relay module desired signal (R_d). Meanwhile, the Peltier element's temperature desired signal (T_d) compared with the actual Peltier element's temperature signal (T_a), which is measured by attaching the LM35 temperature sensor directly on the hot side of the Peltier element, as shown in Figure 3.b. Following from there, the compared error signal inters to the PID controller to generate the manipulating signal of controlling the servomotor angular position. In turn, the servomotor drives the voltage regulator to adjust the Peltier element's temperature signal (T_a).

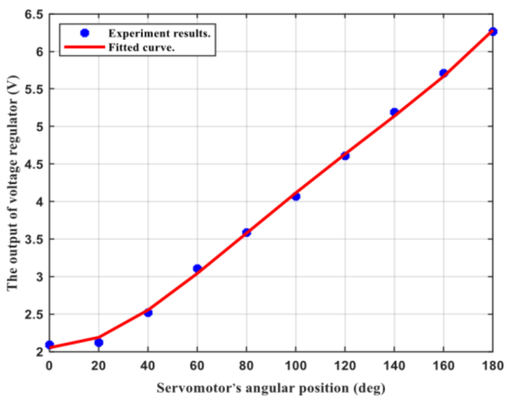

Figure 5: The relation between servomotor angular position regulator output voltage.

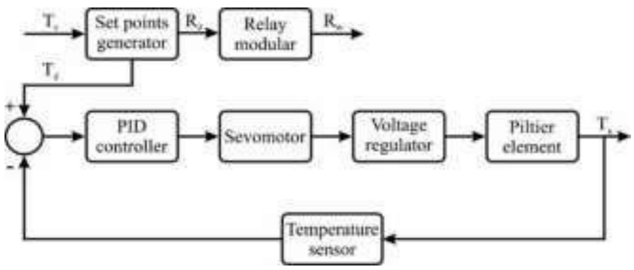

Figure 6: Block diagram of voltage regulator controller. and the

4. The implementation of the arm's withdrawal reflex

Withdrawal reflexes are a relatively new addition to the growing arsenal of producing safe prostheses that aims to reduce the potential for harm to amputees and the prosthetic arm due to collisions, impacts, and painful stimulus. Equipping the prosthetic arm with a tactile temperature sensor and haptic thermal feedback stimulation system for implementing a withdrawal reflex due to the hot noxious stimulus is the main goal of this study. The focus is in particular on the human nociceptive withdrawal reflex (NWR), i.e., the reflex that causes withdrawal from painful stimuli (hot objects or surfaces). Consequently, it enables a range of skills that improves the human-prostheses interaction, both in terms of safety and communication.

However, the hybrid haptic feedback stimulation system presented in this work was examined in two cases based on the range of the object’s temperature, a normal case, and an abnormal case. At the normal case, i.e. when the object’s temperature is below the dangerous threshold, the HHPVFSS will work according to the contact pressure among the prosthetic hand and the clutched object. Meanwhile, the thermal feedback stimulation system will excite the patient’s skin relying on the temperature sensory information, as described in Figure 7 with the green arrows.

When the object’s temperature exceeds the dangerous threshold, the abnormal case will start to implement the withdrawal reflex. Therefore, the microcontroller will block the contact pressure sensory signals and enable the HHPVFSS to work with the temperature signal, in addition to HHTTFSS, as described in Figure 7 with the red arrows.

The single servomotor of the HHPVFSS will excite with a reputational high-frequency sinewave signal that varies from 0-25 degree, in order to rapidly stimulate the user’s skin and inform the brain about absolute necessity to withdraw the prosthetic arm far away from the hot area. For the same reason, the two vibration motors of the HHPVFSS will be stimulated by a pulsing signal varying from 144 – 255 PWM. These fast excitations are completely different from the excitation of the actuators at the normal case. Thus, it is expected that the user of the haptic prosthetic arm will clearly recognize the normal and abnormal cases.

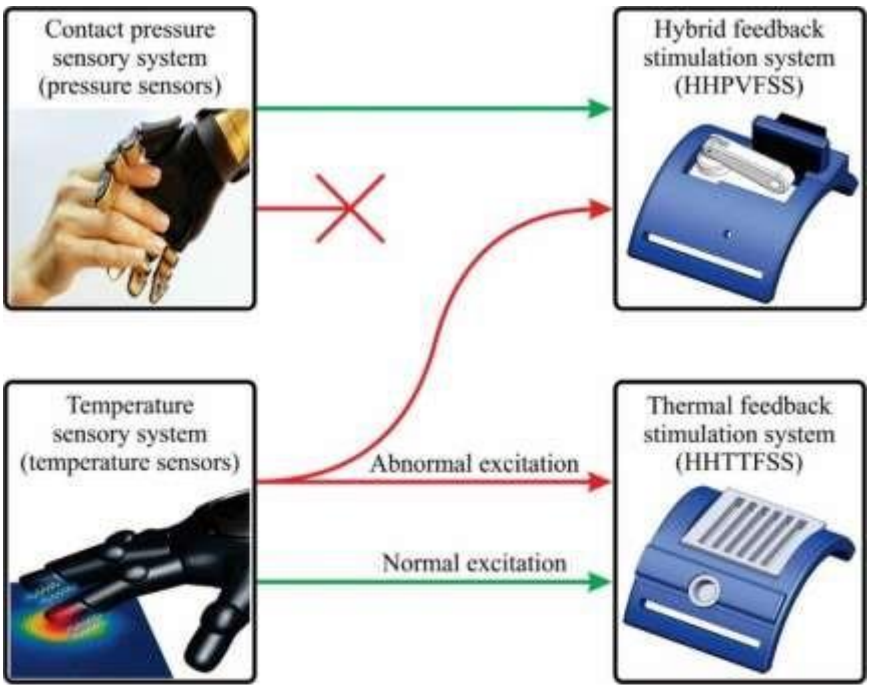

Figure 7: The behavior of the hybrid haptic system under the normal and abnormal operations.

5. Setup and experiment technique

The assessment studies were carried out to ensure that the hybrid haptic wearable device (HHPVFSS and HHTTFSS) operated as expected. The experiments' main three goals include:

(1) to prove the functionality of the designed haptic prosthetic arm to enable its users to implement the withdrawal reflexes in response to the hot noxious stimulus in a quick manner;
(2) To determine whether the hybrid feedback stimulation system can convey tactile information about the surface texture and temperature to the user's brain to the user's brain immediately and without long pre-training requirements; and
(3) to prove the functionality of the hybrid feedback stimulation system to provide tactile information about the surface texture.

The tests were separated into two phases to address all functional features of the system in order to fulfill these objectives. The surface texture detection experiment and the temperature and noxious stimuli detection experiment are the two sections. The amputees' upper limbs were replicated by able-bodied volunteers. The tactile prosthetic arm that presented in the previous study [33] is used in this experiment, as shown in Figure 8. The suggested arm's hybrid tactile sensory system is made up of a rigid base that houses six pressure sensors, one vibration sensor, and two temperature sensors. Six QTC pressure sensors from Peratech[34] with a 10 mm diameter and a 0.1 N to 20 N operational force range were spread throughout the hand for the pressure sensing system.

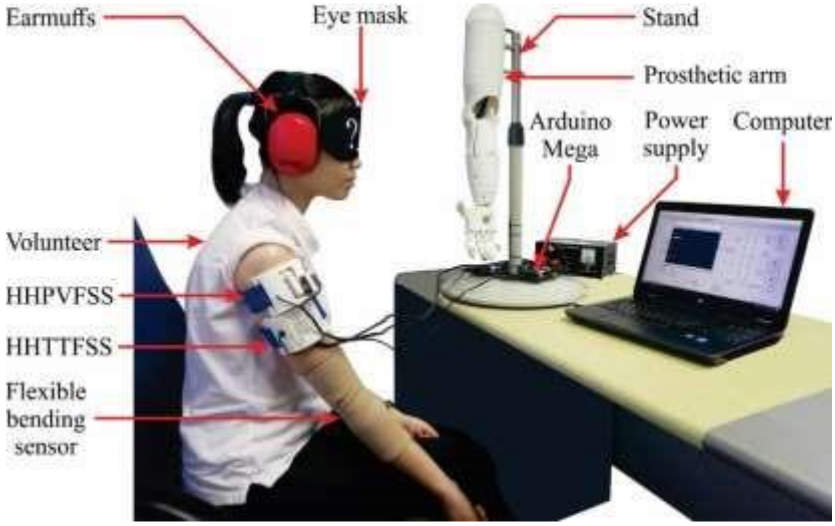

Figure 8: Set-up for the experiment: determining the effectiveness of the haptic wearable device in conveying tactile information.

For the surface texture detection sensory system, a piezoelectric MEAS vibration sensor consisting of a thin strip of piezoelectric material that generates a charge differential when flexed is used to measure subtle vibrational patterns [35]. The sensor was attached to the rear of the index fingertip, in order to record the surfaces tactile information when the finger of the hand slips over different types of surfaces.

Finally, two of LM35 temperature sensors are embedded to the fingertip of the middle and thumb finger. The LM35 series are precision integrated-circuit temperature devices with an output voltage linearly proportional to the Centigrade temperature. It allow measurements with a thermal gradient of less than 0.1 °C, and ±0.5°C accuracy from -55°C to +150°C [36].

The prosthetic arm and computer were placed on the table in all assessment trials, and the healthy volunteers were sitting against the table in a full rest posture, as illustrated in Figure 8. The HHPVFSS and HHTTFSS were mounted on the volunteers’ right upper arm. Furthermore, the flexible bending sensor of the tracking system, which presented in the previous study [33], was fitted to the volunteers’ elbow joint to measure its movements. Lastly, an eye mask and earmuffs were used to block the participants' vision and hearing, preventing this information from impacting their perception.

5.1 Surface texture detection experiment

Three surface textures (sand, stone, and matchsticks) of different roughness were chosen to perform the surface texture detection experiment. The experiment seek to confirm whether the volunteers are able to discriminate the surface textures with the associated vibration patterns of the HHTTFSS. The experiment consists of two phases, i.e. a training phase and an evaluation phase.

During the training phase, a virtual excitation signal was generated to train the volunteers with a completely vision feedback and haptic feedback information. The excitation signals changed between sand, stone, and matchsticks surfaces, in addition to the notouch case by mean of three repetitions per each case and 8 seconds per each step, as described in Figure 9. During the training phase, the textures vary from no feeling (no touch) to smooth (sand) to coarse (stone) and very coarse (matchsticks) and the volunteers have to get used with the excitations by mean of the vision and haptic feedback information.

During the evaluation phase, virtual and real excitations in a random sequence were utilized to examine the ability of the volunteers to discriminate the surface texture. The virtual excitation is comparable to the training stage excitation, whereas for the actual excitation, the prosthetic index finger was allowed to slide over a rotatable platter with three various textured surfaces. Every time, the volunteers were asked what are the type of surface they thought that the artificial finger was touching and sliding on.

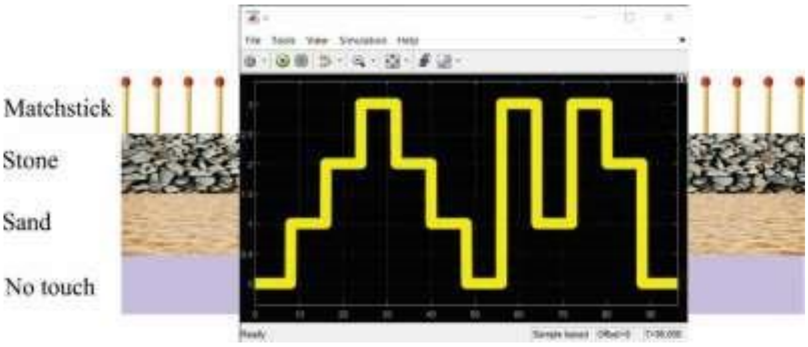

Figure 9: A virtual training phase surface texture excitation.

5.2 The temperature and noxious stimulus detection experiment

The objectively verifying the usefulness of the thermal FSS to assist the users of the prosthetic arm to distinction of the temperature sensory information is the first goal of this experiment. Meanwhile, examining the adaptability of the thermal FSS to help the users of the prosthetic arm to perform the withdrawal reflexes in response to the nociceptive stimuli applied is the second goal of the experiment. Therefore, the temperature and noxious stimulus detection experiment is designed to examine the ability of the volunteers to identify the difference between the temperature levels, namely, a temperature difference threshold. Here, the difference threshold means a change in the temperature that the user can recognize using the thermal FSS.

Firstly, four temperature states (room, warm, hot, and dangerous) were chosen to represent the temperature thresholds in this study. Accordingly, the volunteers were invited to correctly recognize between these thresholds. Therefore, the tactile temperature threshold must be specified. Then, the feedback stimulation temperatures of the thermal FSS regarding each individual tactile temperature threshold have to be determined. Consequently, a primary experiment was performed with 10 healthy volunteers to determine the ranges of the temperature states from the human point of view.

Depending on the results of the experiment, the touching temperature thresholds were ranged as follow: the room threshold (< 30 ℃), the warm threshold ($30 - 42$ ℃), the hot threshold ($42 - 52$ ℃), and the dangerous threshold (> 52 ℃). On the other hand, the temperature of the thermal FSS regarding each temperature state were determined as follows: the room threshold (29 ℃), the warm threshold (35 ℃), the hot threshold (38 ℃), and the dangerous threshold (> 39 ℃).

Returning to the main temperature and noxious stimulus detection experiment, the virtual and real excitation were used to perform the experiment. Figure 10 describes the used virtual excitation, where the virtual sensory signal was programmed to increase step by step from 25 ℃ $-$ 35 ℃ $-$ 45 ℃ $-$ 55 ℃, by the mean of 20 seconds excitation time for the room and dangerous thresholds, and 30 seconds excitation time for the warm and hot thresholds. The same technique used in the temperature thresholds specification's experiment, see Figure 10, was utilized to generate the real excitation. Hence, the mug of varying temperature water was placed closer to the prosthetic hand and the examiner must monitor the reading of the temperature sensor to know the threshold of the current mug's temperature and compare it with the volunteers' answers.

For the room, warm and hot thresholds excitations, the volunteers were asked to quickly indicate the name of the excitation threshold. Meanwhile, a withdrawal reflex action must be done to represent the volunteers' identification due to the dangerous threshold, as shown in Figure 11. Also, when the tactile temperature sensors measured the object's temperature being more than 52 ℃ or the virtual sensory signal reached 55 ℃, the computer system works on exciting the actuators of HHPVFSS to stimulate the volunteers' brain. The brain recognizes the noxious stimulus and orders the healthy arm's muscles to implement a fast withdrawal reflex.

In turn, the flexible bending sensor records the angular movement of the healthy arm's elbow joint and exports it to the computer system. Accordingly, the prosthetic arm will receive order to perform a quick withdrawal reflex by mean of the elbow joint's servomotors. Then, the potentiometer sensor measures the withdrawal reflex and send its signal to the computer system.

A real-time Matlab code was programmed to instantly compare the excitation temperature signal, flexible bending sensor's signal, and the potentiometer sensor's signal. Lastly, the examiner analyses the output plot to decide if the volunteers performed the withdrawal reflex in a quick manner or not and records the responses times.

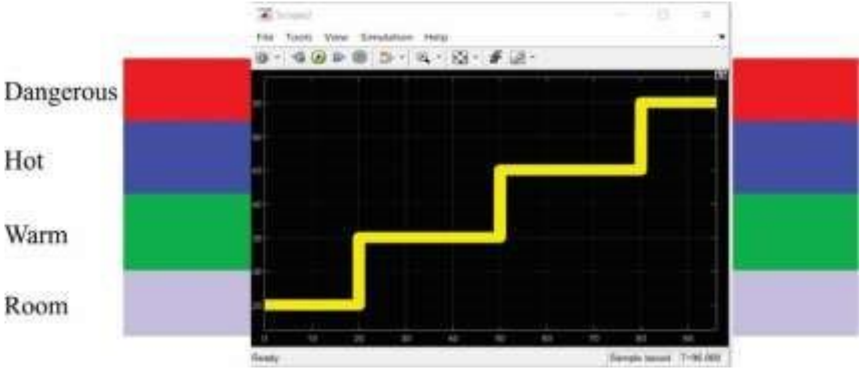

Figure 10: A virtual varying temperature thresholds excitation.

6. Results and discussion

The results are divided into four parts: tracking system evaluation for elbow joint, evaluation of the pressure level detection experiment, evaluation of the surface texture detection experiment, and evaluation of the temperature and noxious stimulus detection experiment. In addition, the employer experiences assessment for hybrid haptic feedback stimulation system. It should be noted that entire results were collected, analyzed, and plotted using the Matlab 2018b program.

6.1 Assessment of pressure rate recognition experiment

Figure 12 depicts the interactions between both the excitations of the vibration and pressure (FSS) of the (HHPVFSS) as a result of an increase in the pressure's biggest immediate sensory signal. As shown in Figure 12.a, the HHPVFSS wearing device's actuators' programmed excitation signals are modeled versus the simulation time (t) whenever the pressure's maximal immediate the sensory signal (u(t)) grows linearly from (0) to (5 Volts) throughout the (5) second of the simulation period. The pressure sensor excitation signal FSS (p(t)) will then grow correspondingly from 0 to 25 degrees Equation (2), as shown in Figure 12.b.

$$p(t) = u(t) \times \left({}^{25}/_{5}\right) \tag{2}$$

The excited signal of the two vibration motors of the vibration FSS (v(t)) is shown in Figure 12.c, which is caused by a rise in the u(t), which is programmed as follows:

$$v(t) = u(t) \times g(t) \times \left({}^{115}/_{5}\right) + 140 \tag{3}$$

where $g(t)$ specifies the pulsing producer indicator. In fact, it's a square-wave signal with unity amplitude, a 0.3-second duration, as well as a pulse width of 50%. As a result, the vibration begins to fluctuate as a square-wave with value varies from (140) to (255) PWM, since the vibration's power is very small, i.e. insensible, at 140 PWM, but 255 PWM is the maximum power allowed for operation for the (LRA) vibrating motors.

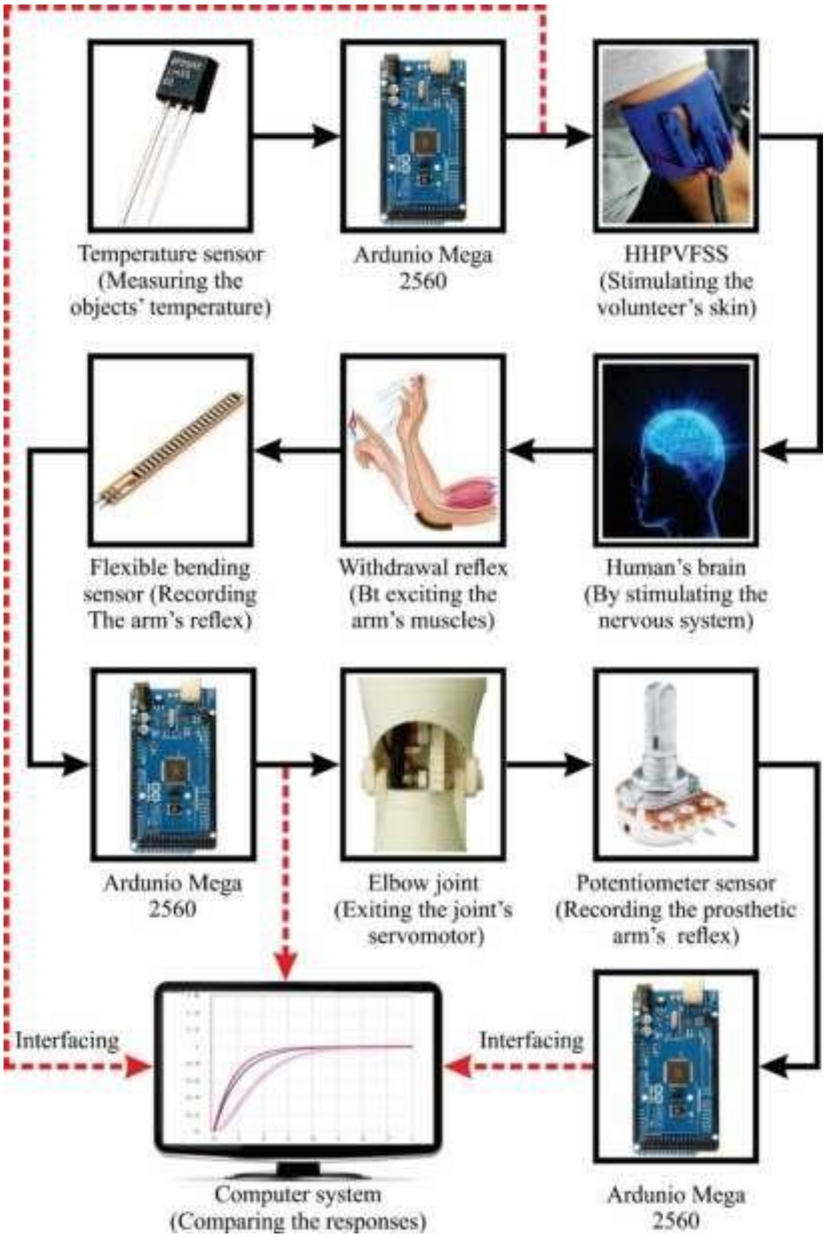

Figure 11: The experiment procedures of noxious stimulus detection.

The excitation signals of the actuators were verified and compared with the virtual pressure sensory signal in order to analyze the actuators' performance of the vibration and pressure (FSS) during the examination of the pressure threshold detection experiment. Figure 13.a shows the four levels of the virtual pressure signal: 0 Volt (no touch), 1.5 Volt (light pressure), 3 Volts (medium pressure), and 5 Volts (heavy pressure). As a result, the pressure FSS's excitation signal alters in order to cause the servomotor to shift its position, as follows: Figure 13.b shows the pressure levels at 0 degrees (i.e. no- touch), 7.5 degrees (i.e. light pressure), 15 degrees (i.e. medium pressure), and 25 degrees (i.e. high pressure). However, the vibration FSS's vibration motors are activated by a square-wave, as shown in Figure 13.c: 0 PWM (no touch), 140 to174.5 PWM (light pressure), 140 to 204 PWM (medium pressure), and 140 to 255 PWM (heavy pressure). The results reveal that when the pressure sensory signal changes, the pressure and vibration excitation signals vary as well.

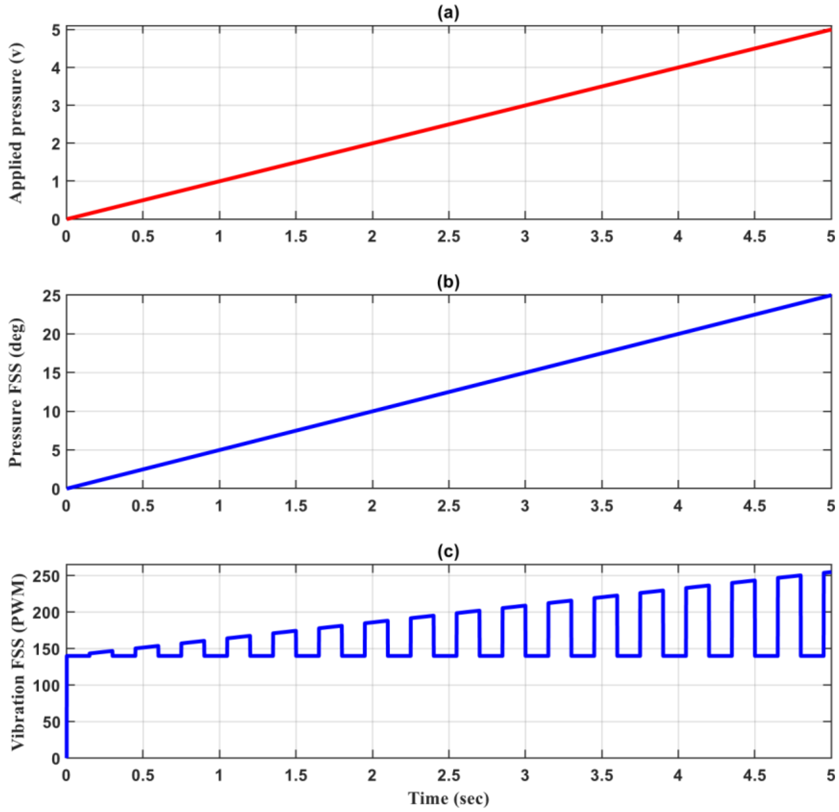

Figure 12: The relationship among the excitations of the pressure and vibration (FSS) and the maximum instant sensory signal.

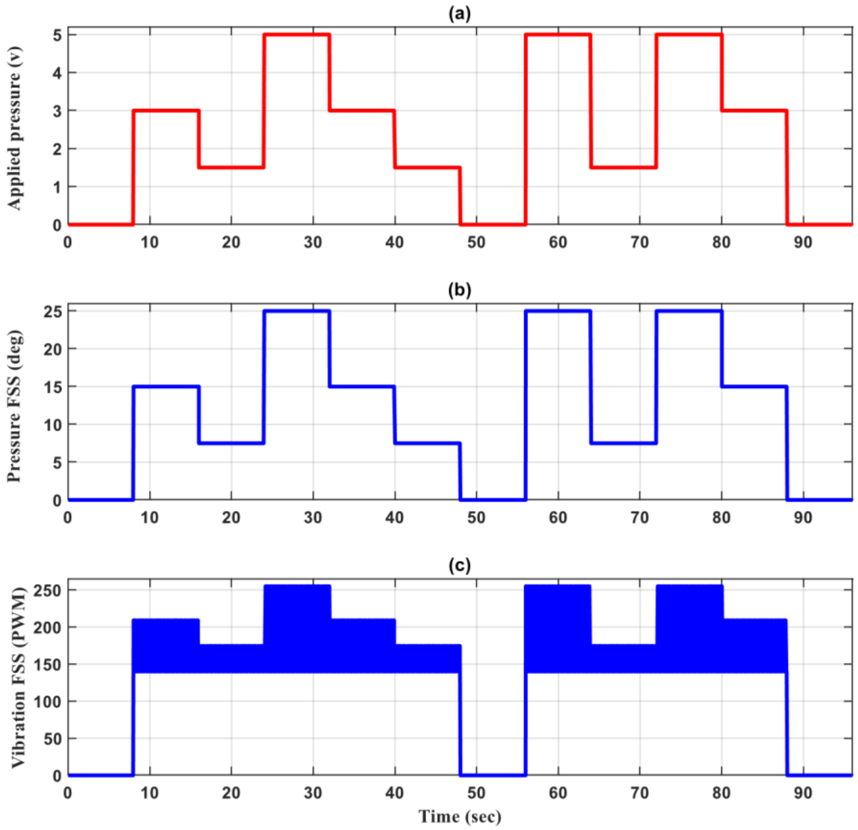

Figure 13: The pressure level detection experiment's assessment findings.

6.2 Assessment of surface texture detection experiment

Different excitation signals were provided to the LRA vibration motors of the surface texture FSS to convey the tactile vibration sensory information regarding the three surfaces (sand, stone, and matchsticks) to the volunteers' brain. A constant excitation of 180 PWM was used to represent the sand surface, in order to provide smooth and continues vibration stimulation to the skin of the user's upper arm, as shown in Figure 14.a. For the stone surface, a square-wave signal of 180 PWM amplitude, and 0.5 second period time with 50% pulse width was used to excite the volunteers with interrupting stimulating, see Figure 14.b. Meanwhile, another square-wave signal of 180 PWM amplitude, 1 second period time, and 15% pulse width was generated to simulate matchsticks surface, where the vibration pulse repeats from time to time, as displayed in Figure 14.c. The final design of these excitation signals was based on several trials of primary experiments, in order to produce three types of frequencies, which are easy for the users to recognize.

The actuator's excitation signal was established relative to the virtual vibration sensory. The main purpose of this validation test is to evaluate the operability of the LRA vibration motor of the surface texture FSS during the evaluation of surface texture detection experiment. Figure 15.a represents the virtual vibration signals, which varies between four different cases. i.e. no touch, sand, stone, and matchsticks, while the excitation signal relative to the surfaces' roughness is described in Figure 15.b. The results clearly indicated that the excitation signal equals to 0 PWM and 180 PWM at the no touch and sand surface, respectively. Moreover, the excitation signal appears as a square-waves varying from 0 to 180 PWM for the stone and matchsticks surfaces, but in different frequencies.

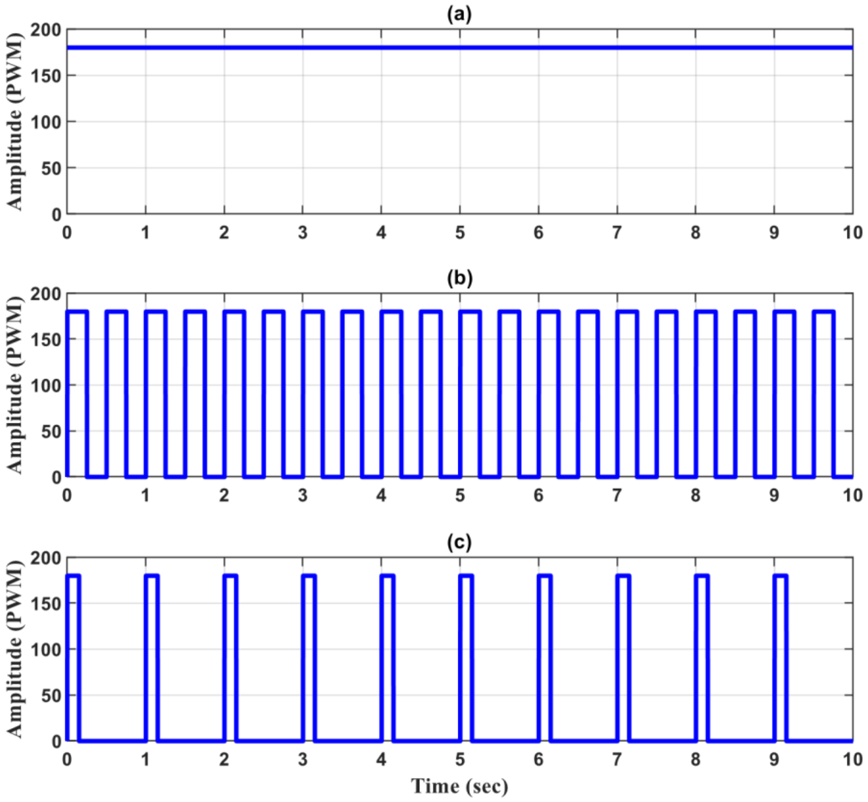

Figure 14: The excitations signals of the surface texture FSS.

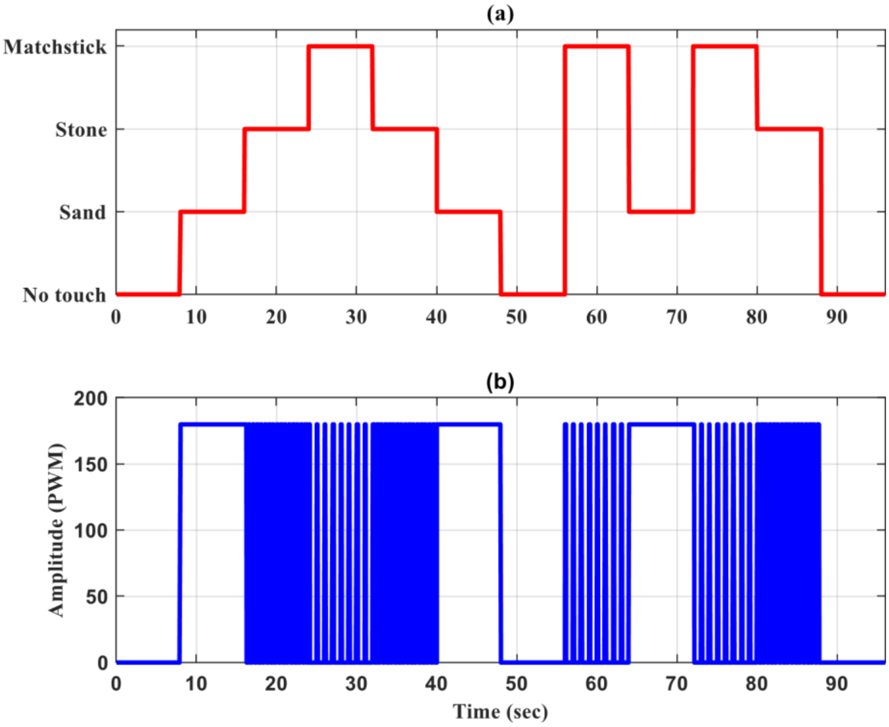

Figure 15: The Result of the experiment on the detection of surface textures.

6.3 Temperature and noxious stimulus detection experiment evaluation

The HHPVFSS was designed to work at the abnormal thermal noxious stimulus. However, the design of the pressure and vibration excitation signal at the abnormal stimulation was highly required. The haptic feedback stimulation system was designed to change its operation cases, normal or abnormal, depending on the value of the dangerous signal (d(t)). The dangerous signal is a conditional signal which has a value of 0 or 1, generated relating to the measured temperature sensory signal (T_s), as follows:

$$d(t) = \begin{cases} 0, & T_s(t) < 52℃ \\ 1, & T_s(t) \geq 52℃ \end{cases} \tag{4}$$

Figure 16.a shows the dangerous signal (d(t)) during 2 sec stimulation time. Accordingly, when the amplitude of the dangerous signal increased from 0 to 1 at 0.5 sec of the simulation time, the excitation signals of the pressure (p(t)) and vibration (v(t)) feedback stimulation system will generate a rapid sine wave, as follows:

$$p(t) = |5 \times \sin(15.t)| \times 5 \tag{5}$$

$$v(t) = |5 \times \sin(15.t)| \times \left({}^{115}/_{5}\right) + 140 \tag{6}$$

Here, the servomotor signal of excitation of the pressure FSS varies from 0 to 25 degrees, as shown in Figure 16.b. Meanwhile, the two vibration motors signal of the vibration (FSS) fluctuating from 140 to 255 PWM, as presented in Figure 16.c.

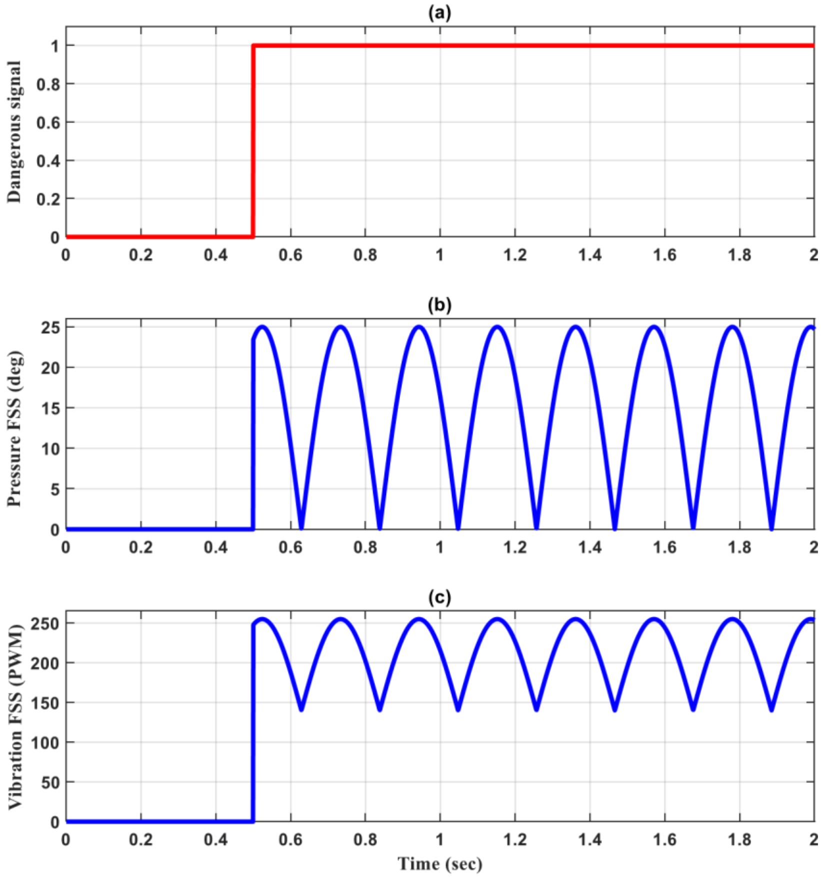

Figure 16: The correlation between the pressure as well as vibration FSS excitations and the hazardous signal.

An example of the evaluation of temperature and noxious stimulus detection experiment is shown in Figure 17 where the red plots denote the input sensors signals while the blue plots indicate the controller or excitation signals. Figure 17.a shows the virtual temperature sensory signal, which is changed in the order of room (first step), warm (second step), hot (third step), and dangerous (fourth step). Hence, the relay modular controller signal will be active at the warm and hot periods, and idle at the rest of stimulation time, see Figure 17.b. Furthermore, Figures 17.c and 17.d describe the amplitude and the behaviors of the excitation servomotor controller signal and the voltage regulator output signal, respectively. At the warm state, the applied voltage to the thermal FSS was quickly increased from 0 V to 6 V and then linearly reduced to 3 V. This behavior of the controller's signal returns to the fact that the temperature of the Peltier element stays in constant increasing when a constant voltage is applied. Therefore, the controller reduces the applying voltage to equilibrium the temperature's increasing behavior, then, keep the temperature of the Peltier element at the constant value as much as possible. Furthermore, at the hot state, the slop of the applied voltage to the thermal FSS has been reduced and the applied voltage ended at 4.5 V, in order to keep the temperature of the Peltier element at the hot state higher than the temperature at the warm state.

After the regulator voltage (the input voltage to the Peltier element) increased, the thermal FSS will follow this occurring change, as shown in Figure 17.e. The figure shows that the temperature of the Peltier element, which is measured by the attached LM35 temperature sensor, changed according to the state of the excitation, as follows: ≈ 29℃ at the room and dangerous states, ≈ 35℃ at the warm state, and ≈ 38℃ at the hot state. It can be noted that the signal of the temperature sensor has continues oscillation because the LM35 temperature sensor is connected with the Peltier element at the same electronic circuit. However, the semiconductor material of the Peltier element give effects on the circuit's voltage and make it instable. In turn, the analog reading of the temperature sensor is affected with this instability behavior.

When the thermal noxious stimulus occurred after 80 sec of the stimulation time (starting of the dangerous zone), the stimulators of the pressure and vibration FSS were rapidly activated and stimulated the skin of

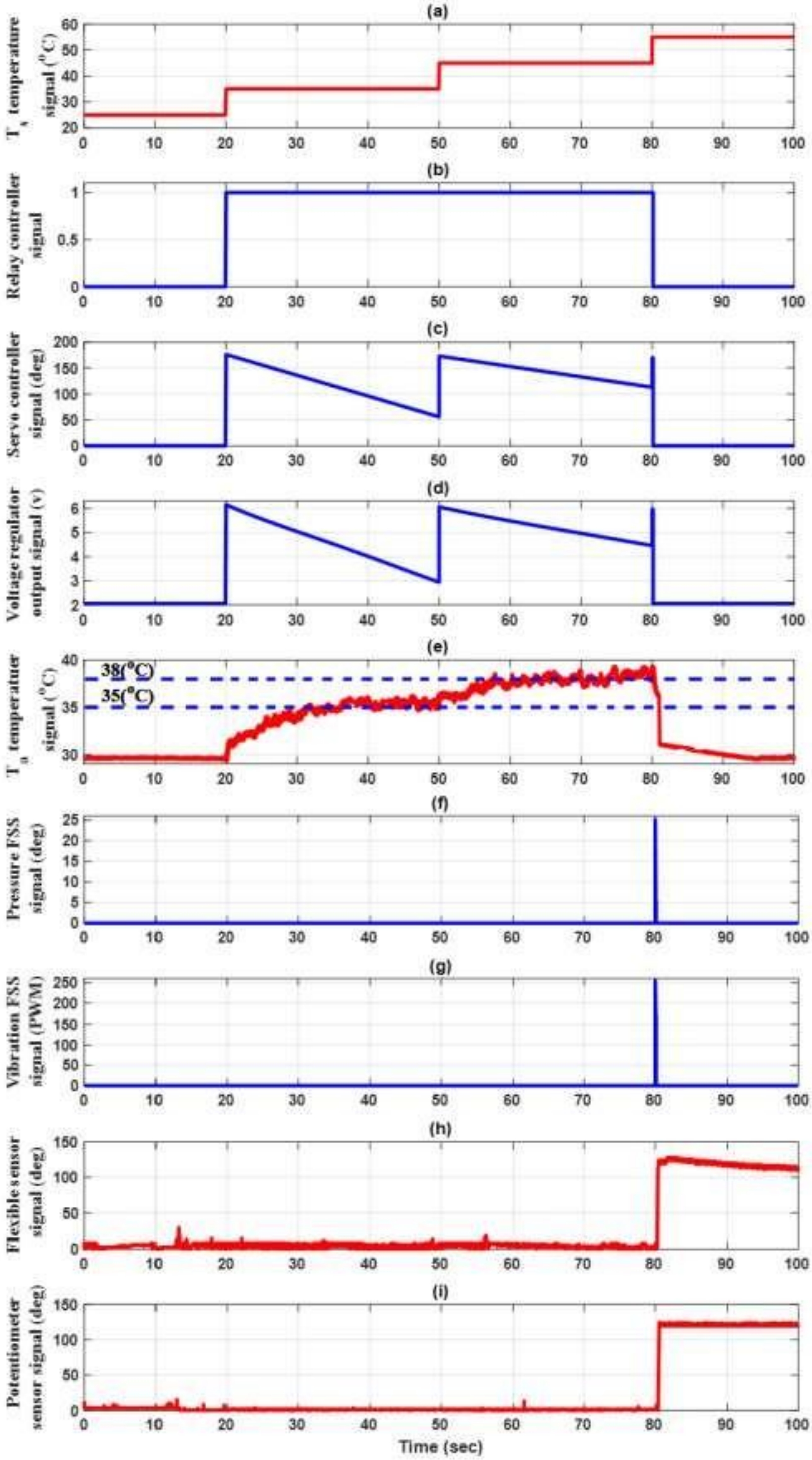

Figure 17: Results from the experiment evaluating temperature and noxious stimuli.

the user's upper limb, as shown in Figures 17.f and 17.g. Then, the user's brain recognizes the dangerous excitation and ordered the healthy arm's muscles to quickly implement the withdrawal reflex, which is measured by the flexible bending sensor as described in Figure 17.h. Subsequently, the tracking system derives the prosthetic arm to perform the withdrawal reflex too. The reflexing of the prosthetic arm was measured by the potentiometer sensor of the elbow joint, as shown in Figure 17.i.

Finally, we study the behavior of the tracking system when implementing the withdrawal reflex due to the thermal noxious stimulus as presented in Figure 17. The focusing period which covers 2 sec from 79 sec to 81 sec of the simulation time is presented in Figure 18. The results show that the value of the temperature sensor signal rapidly increased from $45℃ - 55℃$, i.e. from the hot state to the dangerous state when the simulation time equaled to 80 sec. In turn, the volunteer performed the withdrawal reflex when the simulation time reached 80.32 sec. This implies that there is only a 0.32 sec delay time between the two actions and sequentially involves the following: generate the dangerous conditional signal from the controller system, excite the pressure and vibration FSS, stimulate the volunteer's skin, convey the information to the volunteer's brain, order the healthy arm's muscles, and implement the withdrawal reflex. In addition, it can be noted from the same figure that the prosthetic arm performed the withdrawal reflex when the simulation time equaled to 80.4 sec. Therefore, it can be concluded that there is a 0.08 sec lost time between the two volunteer's response and the prosthetic arm's response due to the thermal noxious stimulus. In general, the entire system seems extremely fast and functional.

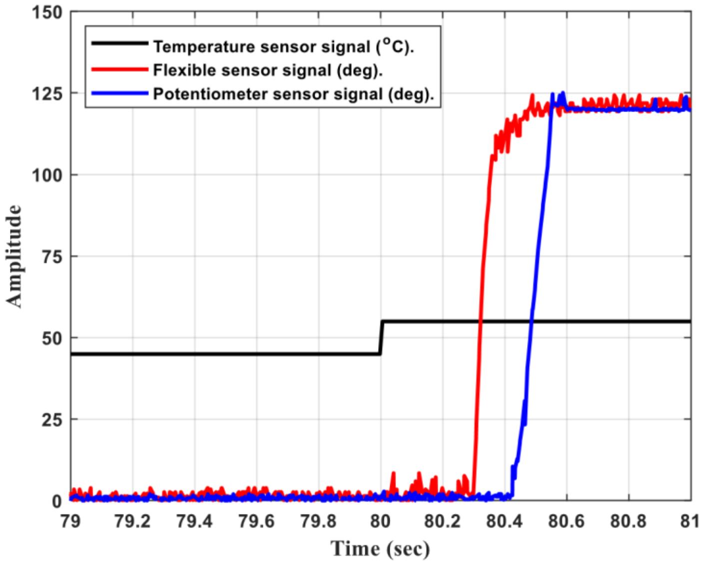

Figure 18: The behavior of the tracking system during implementation of the withdrawal reflex.

6.4 Evaluation of the user experience

Four studies were used to assess the hybrid haptic wearable device's functioning and efficacy. The participants' capacity to perceive touch, begin of contact, end of the touch, grab, slippage, pressure level, surface texture, temperature level, and thermal unpleasant stimuli is tested in these four trials. Figure 19 depicts the evaluation findings in terms of stimulus identification rate (SIR). During the assessment studies, the SIR shows the detection accuracy rate of the volunteers' responses.

The volunteers achieved a 100% accuracy in detecting touches, the start of touches, and the end of touches, and grabbing items in the contact pressure detection studies, whereas 94 percent of the slipping stimulus was effectively replied by the participants. The data was gathered over the course of 120 stimuli for each one of the detection case (40 volunteers and three stimuli for each case). The statistical analyses were carried out by recording the volunteer's response, which was yes for right detection and no for incorrect detection. The rate of accurate responses was then computed for the whole set of stimulus responses. The high recognition precision reflect to the hybrid haptic pressure - vibration feedback stimulator system's exceptional capacity to transfer tactile contact pressure data to the user's brain with high responsiveness, little confusion, and no need for pre-training.

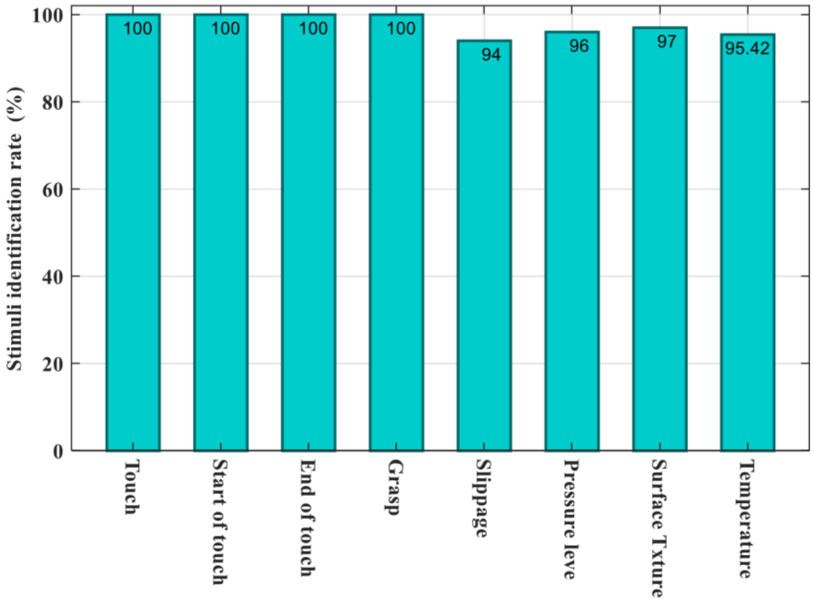

Figure 19: Recognition precision degree of the volunteers' response.

Based on volunteers' responses throughout the tests, the confusion matrix was utilized to assess a collection of the data for the pressure level, surface texture, and temperature level detection investigations. As demonstrated in Figures 20 - 22, it's a way of measuring performance for measuring the correct detection's accuracy answer to the overall detection answer for all stimuli during a single test. The number of accurate replies across the total of stimuli for each excitation goal is represented by the main diagonal of the matrix (pink-cells). The detection accuracy and true positive rates are represented in the matrix's last row and column (light greenish cells). The average accuracy, i.e. SIR, is highlighted in the bottom-right corner (dark green cell). The erroneous responses are represented by the leftover components (white cells).

Figure 20 indicates the confusion matrix for estimating the SIR of the pressure level detection test for the pressure level detection experiment. The letters L, M, and H stand for light, medium, and heavy pressure levels, respectively, while no contact denotes an idle state in which the prosthetic hand does not touch or hold the manipulating items. The number of accurate answers for a total of 120 stimuli for each pressure level is represented by the main diagonal of the matrix (40 volunteers and 3 repetitions). According to the results of the confusion matrix, 96 percent of the pressure levels were correctly recognized. Because the pressing force and vibration frequency fluctuate appropriately with the applied pressure, the change in amplitude can be easily identified; the design of the HHPVFSS wearable gadget completely contributes to this extremely acceptable outcome.

For the surface texture detection experiment, the statistical analysis of calculating the SIR of the surface texture detection experiment is seen in Figure 21. The symbols Sa, St, and Ma refer to sand, stone, and matchsticks surfaces, respectively, while the idle of no touch or grasp state is inscribed by "No touch". The foremost diagonal of the matrix specify to the quantity of exact correct answers with respect to over-all of 120 stimuli per each of the four different surfaces (40 volunteers and 3 repetitions).

According to the confusion matrix of the surface detection test, 97% of the surfaces' stimuli were detected correctly. In addition, it can be noted that the volunteers recorded the lowest detection accuracy with the matchsticks surface, which equals to 91.67%. The design of the vibration motor's excitation signal contributed partially to this result, since the volunteers were confused with the excitation signal of the stone surface or even with the no-touch idle state, as shown in the target surface texture's column of the matchstick surface (fourth column), see Figure 21.

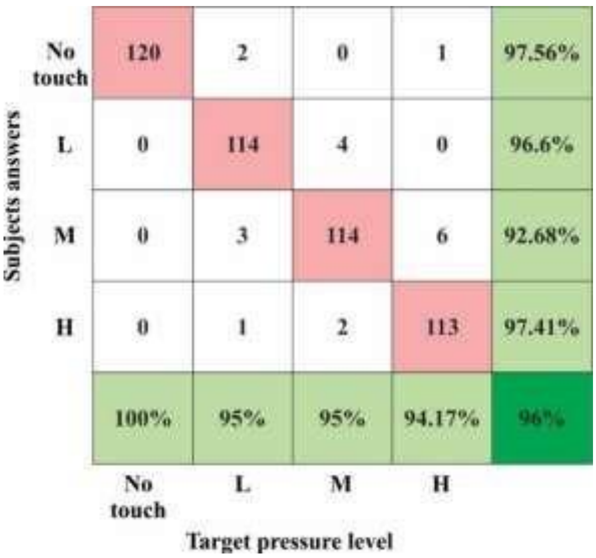

Figure 20: Confusion matrix (pressure level detection experiment).

Figure 21: Confusion matrix (surface texture detection experiment).

Lastly, for the temperature level and noxious stimulus detection experiment, the accuracy matrix was calculated as a ratio of the correct answers reported by volunteers to the total number of trials given per temperature range, as described in Figure 22. All forty healthy volunteers achieved at least 108 successes out of the total 120 stimuli per each temperature threshold (40 volunteers and 3 repetitions per each threshold), equivalent to a minimum of 90 % accuracy in discriminating the dangerous threshold. Moreover, temperature range identification with 100 % in detecting accuracy was satisfied at the room threshold. The average accuracy of indicating correct temperature ranges of the test thresholds across all the volunteers was 95.42 %. The volunteers were consistently able to differentiate between most temperature thresholds by depending on the haptic stimulating of the designed hybrid haptic feedback wearable device. The entire results prove the functionality of the Peltier element's controller. In addition, it evidence the effectiveness of the interfacing between the HHPVFSS and HHTTFSS.

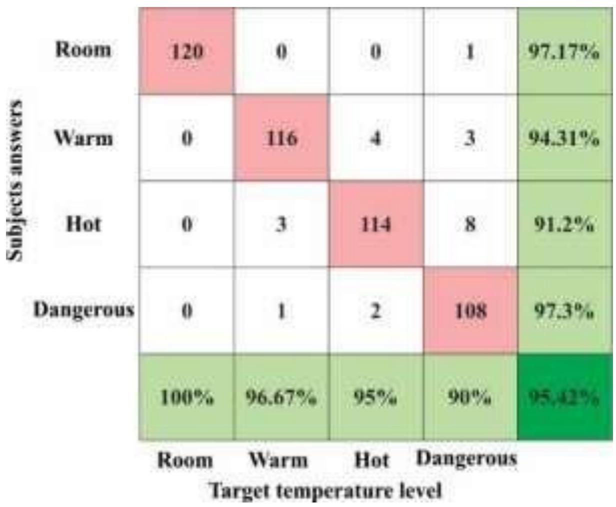

Figure 22: Confusion matrix with the statistical analysis of the temperature and noxious stimulus detection experiment.

7. Conclusion

The novelty of this work is to allow the user to, non-invasively, receive multi direct feedback information from the hybrid tactile sensory system to create more functional and intuitive tactile feedback. Therefore, this study has been conducted to quantitatively determine the effectiveness of these types of haptic displays as a means of conveying sensory information to a prosthesis user. Test subjects in this research endorsed the effectiveness of our proposed design. Accordingly, the results suggest that incorporating the haptic feedback system into advancing prosthetic technology could allow prosthesis users to: (i) enjoy greater dexterity and an increased ability to efficiently complete daily tasks, and (ii) reduce the extreme dependence on visual feedback during contacting or manipulating objects.

To our best knowledge, this is the first attempt to design and evaluate a thermal haptic feedback stimulation system has the ability to assist the operator of the haptic prosthetic arm to implement a withdrawal reflex due to the thermal noxious stimulus.

The haptic device's capacity to stimulate the human nervous system was tested using forty able-bodied participants in the assessment. The results revealed that all of the volunteers were able to distinguish between the sensation of touch, the start of contact, the end of touch, and gripping items appropriately. Meanwhile, 94%, 96%, 97%, and 95.24% of the whole stimuli were positively recognized by the volunteers throughout the experiments of slippage, pressure level, surface texture, and temperature, respectively. In addition, the results proved the capability of the haptic system to excite the human brain about abnormal noxious stimulus and make the volunteers perform a quick withdrawal reflex within 0.32 sec.

Based on the assessment results and the participants' experiences, the study's general conclusions and recommendations are as follows:

1. It is possible to recover the missing feeling to the amputees, whom unfortunately lost, partially or entirely, their upper arm, by non-invasively stimulating the skin of the remaining parts from the amputees' arms or any other spots on their bodies.
2. The capability of the proposed haptic feedback stimulation system to convey the huge tactile information to the users' brain without the brain's confusion or requiring long hours of pre-training.
3. The ability of the designed tactile prosthetic arm and its hybrid haptic feedback system to perform new tactile tasks like the withdrawal reflex near as possible to the activity of the real healthy arm.
4. The proposed tactile prosthetic arm and the haptic feedback system have low cost and its entire tools are available on the market.
5. The final size of the haptic wearable device depends completely on the user's body size and degree of the comfort feeling.
6. The temperature thresholds and the temperature of the thermal FSS depend essentially on the user of the upper limb prostheses, therefore, it should be set according to a primary experiment on the user himself.
7. The Peltier element was designed to work with 6 V as a maximum applying input voltage because applying high voltage is undesirable. It makes the element to consume large amounts of current that would quickly drain the prosthesis' battery.

8. References

[1] L. J. Marks and J. W. Michael, "Science, medicine, and the future: artificial limbs," BMJ: British Medical Journal, vol. 323, p. 732, 2001.

[2] M. Yoshikawa, Y. Taguchi, S. Sakamoto, S. Yamanaka, Y. Matsumoto, T. Ogasawara, et al., "Trans-radial prosthesis with three opposed fingers," in Intelligent Robots and Systems (IROS), 2013 IEEE/RSJ International Conference on, Tokyo, Japan,, 2013, pp. 1493-1498.

[3] D. J. Atkins, D. C. Heard, and W. H. Donovan, "Epidemiologic overview of individuals with upper-limb loss and their reported research priorities," JPO: Journal of Prosthetics and Orthotics, vol. 8, pp. 2-11, 1996.

[4] V. Klinge, "Effects of exteroceptive feedback and instructions on control of spontaneous galvanic skin responses," Psychophysiology, vol. 9, pp. 305-317, 1972.

[5] R. E. Prior, J. Lyman, P. A. Case, and C. M. Scott, "Supplemental sensory feedback for the VA/NU myoelectric hand. Background and preliminary designs," Bull Prosthet Res, vol. 10, pp. 170-91, 1976.

[6] M. N. Nemah, C. Y. Low, O. H. Aldulaymi, P. Ong, and A. A. Qasim, "A Review of Non-Invasive Haptic Feedback stimulation Techniques for Upper Extremity Prostheses," International Journal of Integrated Engineering, vol. 11, 2019.

[7] L. Zollo, S. Roccella, E. Guglielmelli, M. C. Carrozza, and P. Dario, "Biomechatronic design and control of an anthropomorphic artificial hand for prosthetic and robotic applications," IEEE/ASME Transactions On Mechatronics, vol. 12, pp. 418-429, 2007.

[8] B. B. Edin, L. Beccai, L. Ascari, S. Roccella, J.-J. Cabibihan, and M. C. Carrozza, "Bio-inspired approach for the design and characterization of a tactile sensory system for a cybernetic prosthetic hand," in Proceedings 2006 IEEE International Conference on Robotics and Automation, 2006. ICRA 2006., 2006, pp. 1354-1358.

[9] C. Cipriani, F. Zaccone, S. Micera, and M. C. Carrozza, "On the shared control of an EMG-controlled prosthetic hand: analysis of user–prosthesis interaction," IEEE Transactions on Robotics, vol. 24, pp. 170-184, 2008.

[10] R. E. Fan, M. O. Culjat, C.-H. King, M. L. Franco, R. Boryk, J. W. Bisley, et al., "A haptic feedback system for lowerlimb prostheses," IEEE Transactions on Neural Systems and Rehabilitation Engineering, vol. 16, pp. 270-277, 2008.

[11] A. Chatterjee, P. Chaubey, J. Martin, and N. V. Thakor, "Quantifying prosthesis control improvements using a vibrotactile representation of grip force," in 2008 IEEE Region 5 Conference, 2008, pp. 1-5.

[12] H. Huang, T. Li, C. Antfolk, C. Enz, J. Justiz, and V. M. Koch, "Experiment and investigation of two types of vibrotactile devices," in Biomedical Robotics and Biomechatronics (BioRob), 2016 6th IEEE International Conference on, Singapore, Singapore, 2016, pp. 1266-1271.

[13] P. Kapur, M. Jensen, L. J. Buxbaum, S. A. Jax, and K. J. Kuchenbecker, "Spatially distributed tactile feedback for kinesthetic motion guidance," in Haptics Symposium 2010, Waltham, Massachusetts, 2010, pp. 519-526.

[14] J. Wheeler, K. Bark, J. Savall, and M. Cutkosky, "Investigation of rotational skin stretch for proprioceptive feedback with application to myoelectric systems," IEEE Transactions on Neural Systems and Rehabilitation Engineering, vol. 18, pp. 58-66, 2010.

[15] M. D'Alonzo, F. Clemente, and C. Cipriani, "Vibrotactile stimulation promotes embodiment of an alien hand in amputees with phantom sensations," IEEE Transactions on Neural Systems and Rehabilitation Engineering, vol. 23, pp. 450-457, 2015.

[16] M. C. Jimenez and J. A. Fishel, "Evaluation of force, vibration and thermal tactile feedback in prosthetic limbs," in Haptics Symposium (HAPTICS), 2014 IEEE, Houston, TX, USA, 2014, pp. 437-441.

[17] M. R. Motamedi, J.-P. Roberge, and V. Duchaine, "The Use of vibrotactile feedback to restore texture recognition capabilities, and the effect of subject training," IEEE Transactions on Neural Systems and Rehabilitation Engineering, vol. 25, pp. 1230-1239, 2017.

[18] S. Fukushima, H. Sekiguchi, Y. Saito, W. Iida, T. Nozaki, and K. Ohnishi, "Artificial Replacement of Human Sensation Using Haptic Transplant Technology," IEEE Transactions on Industrial Electronics, vol. 65, pp. 3985-3994, 2018.

[19] K. Bark, J. W. Wheeler, S. Premakumar, and M. R. Cutkosky, "Comparison of skin stretch and vibrotactile stimulation for feedback of proprioceptive information," in Symposium on Haptic Interfaces for Virtual Environments and Teleoperator Systems 2008, Reno, Nevada, USA, 2008, pp. 71-78.

[20] C. Antfolk, M. D'Alonzo, M. Controzzi, G. Lundborg, B. Rosén, F. Sebelius, et al., "Artificial redirection of sensation from prosthetic fingers to the phantom hand map on transradial amputees: vibrotactile versus mechanotactile sensory feedback," IEEE transactions on neural systems and rehabilitation engineering, vol. 21, pp. 112-120, 2013.

[21] H. Huang, T. Li, C. Bruschini, C. Enz, J. Justiz, C. Antfolk, et al., "Multi-modal Sensory Feedback System for Upper Limb Amputees," in 2017 New Generation of CAS (NGCAS), Genova, Genoa, 2017, pp. 193-196.

[22] E. Romero and D. Elias, "Design of a non invasive haptic feedback device for transradial myoelectric upper limb prosthesis," in ANDESCON, 2016 IEEE, Arequipa, Peru, 2016, pp. 1-4.

[23] A. Ajoudani, S. B. Godfrey, M. Bianchi, M. G. Catalano, G. Grioli, N. Tsagarakis, et al., "Exploring teleimpedance and tactile feedback for intuitive control of the pisa/iit softhand," IEEE transactions on haptics, vol. 7, pp. 203-215, 2014.

[24] M. N. Nemah, S. S. Khaleel, O. H. Aldulaymi, C. Y. Low, P. Ong, and B. A. Jabbar, "A Wearable Hybrid Haptic Feedback Stimulation Device for Upper Limb Prostheses," International Journal of Mechanical and Mechatronics Engineering (IJMME), vol. 19, pp. 104-114, 2019.

[25] M. Abdollahpour, "Design of an experiment to calibrate a peltier element and measuring thermal conductivity," Eastern Mediterranean University (EMU)-Doğu Akdeniz Üniversitesi (DAÜ), 2014.

[26] D. P. PVT.LTD. RAISE 3D N2 PLUS. Available: https://www.ithink3dp.com

[27] A. M. Donald and E. J. Kramer, "Plastic deformation mechanisms in poly (acrylonitrile-butadiene styrene)[ABS]," Journal of Materials Science, vol. 17, pp. 1765-1772, 1982.

[28] OnlineShop. (2018). Micro Servo 5-10g / SG90 Analog. Available: http://www.towerpro.com.tw

[29] PrecisionMicrodrives. (2018). 10mm Linear Resonant Actuator. Available: https://www.precisionmicrodrives.com

[30] HB Brand Electronic Components. (2019). Thermoelectric Cooler TEC1-12706. Available: www.hebeiltd.com.cn

[31] Texas Instruments. (2011). Linear and Switching Voltage Regulator Fundamentals. Available: http://www.ti.com/lit/an/snva558/snva558.pdf

[32] Lazada. (2019). 1 Channel 5V Relay Module With Optocoupler Protection. Available: https://www.lazada.com.ph/products/1-channel-5v-relay-module-with-optocoupler-protection-i100047427s100061336.html

[33] Mohammed Najeh Nemah, Cheng Yee Low, Annisa binti Jamali, Shahrol Mohamaddan, A. K. Kareem, and O. M. Fakhri1, "Design a hybrid haptic feedback stimulation device for helping the prostheses' patients to recover the sensation," presented at the International Conference on Mechanical & Manufacturing Engineering 2019 (ICME2019), Melaka, Malaysia, 2019.

[34] Peratech. (November 2015). QTC SP200 Series Datasheet SP200-05 Series, Single Point Sensors. Available: https://www.peratech.com

[35] Seed, "Grove - Piezo Vibration Sensor," ed, 2015.

[36] Texas Insrtuments. (2017, December). LM35 Precision Centigrade Temperature Sensors. Available: www.ti.com